Robert H. Kraus Jr.
Michelle A. Espy
Per E. Magnelind
Petr L. Volegov

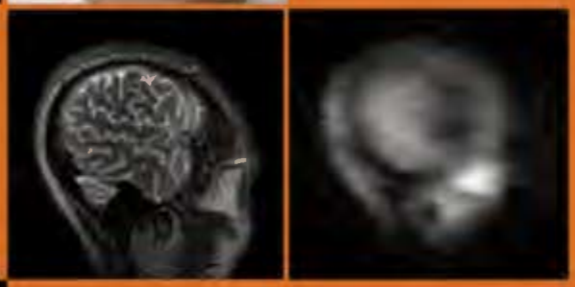

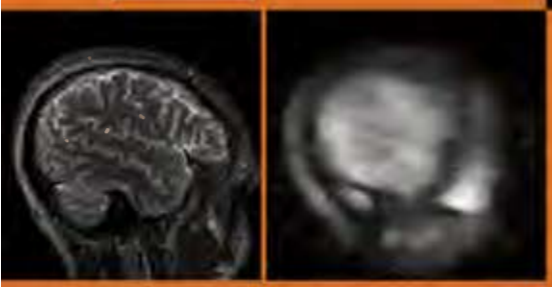

ULTRA-LOW FIELD NUCLEAR MAGNETIC RESONANCE

A NEW MRI REGIME

OXFORD

ULTRA-LOW FIELD NUCLEAR MAGNETIC RESONANCE

ULTRA-LOW FIELD NUCLEAR MAGNETIC RESONANCE

A New MRI Regime

Robert H. Kraus Jr., PhD
Chief Scientist, Samitaur Medical Technologies
Honolulu, HI

Michelle A. Espy, PhD
Scientist, Los Alamos National Laboratory
Los Alamos, NM

Per E. Magnelind, PhD
Scientist, Los Alamos National Laboratory
Los Alamos, NM

Petr L. Volegov, PhD
Scientist, Los Alamos National Laboratory
Los Alamos, NM

OXFORD
UNIVERSITY PRESS

OXFORD
UNIVERSITY PRESS

Oxford University Press is a department of the University of Oxford.
It furthers the University's objective of excellence in research, scholarship,
and education by publishing worldwide.

Oxford New York
Auckland Cape Town Dar es Salaam Hong Kong Karachi
Kuala Lumpur Madrid Melbourne Mexico City Nairobi
New Delhi Shanghai Taipei Toronto

With offices in
Argentina Austria Brazil Chile Czech Republic France Greece
Guatemala Hungary Italy Japan Poland Portugal Singapore
South Korea Switzerland Thailand Turkey Ukraine Vietnam

Oxford is a registered trademark of Oxford University Press in the UK
and certain other countries.

Published in the United States of America by
Oxford University Press
198 Madison Avenue, New York, NY 10016

Library of Congress Cataloging-in-Publication Data
Kraus, Robert H., Jr. (Robert Henry), author.
Ultra-low field nuclear magnetic resonance : a new MRI regime / Robert H. Kraus Jr., Michelle A. Espy, Per E. Magnelind, Petr L. Volegov.
p. ; cm.
Includes bibliographical references and index.
ISBN 978–0–19–979643–4 (alk. paper)
I. Espy, Michelle A. (Michelle Anna), author. II. Magnelind, Per E., author. III. Volegov, Petr L., author. IV. Title.
[DNLM: 1. Magnetic Resonance Imaging. WN 185]
RC78.7.N83
616.07′548—dc23
2013023133

9 8 7 6 5 4 3 2 1
Printed in the United States of America
on acid-free paper

To those who, through science, would help others.

CONTENTS

FOREWORD

A decade ago in Berkeley, it was shown that the nuclear magnetic resonance (NMR) line width of protons in a liquid could be very narrow in a magnetic field B_0 of a couple of microtesla, even though it was deliberately made highly inhomogeneous by the standards of conventional NMR. In fact, the narrow line width was to nobody's surprise; the important point being the high signal-to-noise ratio (SNR) obtained at a Larmor frequency f_0 of 75Hz. This was achieved by combining two well-known ideas: pre-polarization of the proton spins by a much larger magnetic field B_p that was turned off before the NMR signal was acquired, and the detection of the NMR signal with an untuned detector based on a superconducting quantum interference device (SQUID). Most SQUIDs operate at 4.2K, the boiling point of liquid helium. Unlike a Faraday detector, the SQUID has a frequency-independent response to magnetic flux. These early experiments also demonstrated the simplicity of obtaining the spectra of two nuclear species in a single acquisition using switched magnetic fields and of directly detecting the scalar coupling (*J*-coupling) splitting in heteronuclear spin systems—a unique benefit of the SQUID sensor.

Subsequently, the Berkeley group made the logical step to ULF magnetic resonance imaging (ULF MRI) by adding switched field gradients. Their system, built with lumber and copper wire coils, operated in a magnetic field of 132μT, corresponding to f_0 = 5,600Hz, four orders of magnitude lower than in conventional high-field (HF) MRI. The first image was of a pepper slice. Shortly after, an in-plane resolution of 1mm was demonstrated. This was followed by the three-dimensional *in vivo* image of an arm with an in-plane resolution of 2mm. Subsequently, the group demonstrated the strong dependence of the longitudinal relaxation time T_1 on the concentration of agarose gel in water at low fields, in contrast to the weak dependence at high fields. This observation resulted in the development of ULF T_1-weighted contrast imaging. The large skin depth of metals at ULF enabled the imaging of a pepper in a metal container. The requirement of only modest field homogeneity at ULF made possible undistorted images in the presence of a metal bar, which could, for example, be an orthopaedic screw.

Today, groups at perhaps 20 institutions worldwide are involved in some aspect of ULF NMR and ULF MRI. For example, a line width of 0.034Hz was observed in benzene in the Earth's field, and of 0.34Hz in a *J*-coupling spectrum. An early demonstration was the simultaneous acquisition of the stimulated magnetic signal from the human brain (magnetoencephalography [MEG]) and the ULF NMR signal from protons in the brain, using a single SQUID. Although these signals were in no way correlated, this was an important demonstration of the potential to combine the two modalities into a single acquisition system. Three-dimensional *in vivo* images of the brain were acquired with multiple SQUIDs. Trials at the Albuquerque airport showed the ability of ULF MRI in a T_1-contrast imaging

mode to seek out liquids in carry-on luggage. On the technical front, an MRI phantom was successfully imaged using a SQUID on a cryocooler. Alternative sensors to SQUIDs are being explored—for example, "mixed sensors," which combine a superconducting pickup loop with a giant magnetoresistance sensor, and atomic magnetometers.

What are the long-term prospects for this field? In my view, although other as-yet-unheralded applications will undoubtedly emerge, if there is to be a major application it will be in medical imaging. But it will not be easy! HF clinical MRI is a magnificent tool, with perhaps 30,000 machines worldwide. Its great versatility leads to multiple applications, and it can achieve a spatial resolution of 1mm for most parts of the human body in a relative short time. A particular advantage is that specifically designed detection coils—at room temperature—can be placed over any part of the body to optimize detection sensitivity.

What would it take for ULF MRI to compete? It's mostly a question of SNR. The magnetic moment of a given ensemble of spins scales as B_0, and the signal it induces in a tuned pickup coil—by Faraday's law—scales as f_0. Thus, all things being equal, the signal from a tuned detector scales as B_0^2. Given that realizable pulsed pre-polarizing fields are likely to be an order of magnitude lower than the 1.5T field of a clinical system and that ULF MRI involves an untuned detector, the simple fact is that ULF MRI is unlikely to compete with HF MRI in terms of combined speed and spatial resolution. One may argue, with some justification, that a ULF MRI machine is likely to be substantially less costly than a 1.5T machine, but at least in the developed world the radiologist—not to mention the patient—seeks high resolution without an unduly long imaging time. Thus, in my view, if the goal of ULF MRI is to compete head on with HF MRI on its own terms, it is doomed to failure.

Fortunately, ULF MRI has its own virtues that extend beyond raw speed and resolution. An obvious strength is its greatly enhanced T_1 contrast compared with HF MRI. In HF MRI, T_1-weighted contrast imaging is well established but has its limitations. For example, in the case of breast cancer, there is no intrinsic T_1 contrast between cancerous and healthy tissue. This drawback is overcome by injecting a Gd-salt into the bloodstream, which flows preferentially to the tumor. The paramagnetic Gd ions enhance the T_1 relaxation rate, enabling one to image the tumor. Although this technique yields high resolution of the tumor, the rate of false positives has inhibited its becoming a screening technique for breast cancer. The use of the contrast agent works well for brain tumors but not at all for prostate cancer, which is the second leading cause of cancer deaths among American men.

The intrinsic difference in T_1 at low fields for different tissue types has been long known; it is the development of ULF MRI that has enabled one to take advantage of it. Although ULF T_1-weighted contrast imaging is well established in phantoms, in tissue it is in its infancy. Studies at Berkeley on *ex vivo* prostate tissue surgically removed from cancer patients, however, have established that T_1 in tumors is substantially shorter than in normal tissue. Simulations suggest that this T_1 difference is sufficient to produce *in vivo* images with sufficient contrast-to-noise ratio and spatial resolution to be clinically significant. Clearly, only clinical trials can establish the effectiveness of this technique, which relies on the intrinsic difference of T_1. If it were possible to image prostate cancer with ULF MRI, one could hope to use it, for example, to assess the extent of the disease in newly diagnosed patients, to provide a map to guide biopsy should it be deemed necessary, and to monitor changes in the prostate during active surveillance or therapies such as brachytherapy (implantation of radioactive seeds), thereby obviating the need for repeated biopsies. An obvious question is the applicability to other kinds of cancer. Could ULF MRI be used to screen for breast cancer? Or to detect ovarian cancer—which is notoriously difficult to detect at an early stage? Again, only clinical trials can address these questions.

A second forward-looking application of ULF MRI is its combination with systems for MEG. These systems, containing typically 300 SQUIDs, are used to detect stimulated or spontaneous magnetic fields from neurons in the brain in real time. They are used, for example, for presurgical mapping of brain tumors, the locating and presurgical mapping of sites of focal epilepsy, and the progression of recovery from brain trauma such as brain injury or stroke. To interpret the magnetic source image, an MRI of the brain is essential. The MEGMRI project, funded by the European Union and involving about a dozen institutes led by Aalto University, Helsinki, aims to incorporate ULF MRI into MEG systems. In principle, this simply involves the addition of appropriate sets of coils to existing MEG systems. The NMR signals are detected by the array of SQUIDs, so that averaging over these sensors can substantially reduce their noise. The notion of obtaining magnetic source and MR images with a single system is very appealing, since it overcomes difficulties in co-registering images obtained with two different systems and could result in substantial cost savings. In practice, the combination of MEG and MRI has many challenges, but there is every reason to believe these will be overcome. If so, these combined technologies could have a significant impact both clinically and commercially.

Currently, the holy grail of ULF MRI is its potential for direct neural current imaging (DNI). The essential idea is that currents flowing in neurons during neural activity produce local magnetic fields that can induce a tiny shift in the phase of the NMR signal over a tiny region. Strenuous efforts have been expended to observe this effect in HF MRI, so far without success. Since ULF MRI operates at a magnetic field four orders of magnitude lower, one expects the relative shift of the NMR signal to be enhanced by the same factor. The realization of DNI would be revolutionary, making real-time, spatially localized observation of neural activity a reality.

What are the challenges in bringing ULF MRI to clinical practice? The single biggest issue is, again, SNR, which scales as the ratio of the NMR signal at the sensor to the noise at the sensor, B_N. The imaging time for a given spatial resolution sales inversely as $(SNR)^2$, and hence as B_N^2/B_p^2. This immutable law should be displayed prominently in every ULF MRI laboratory! To obtain a sensible imaging time, one requires a sensor noise approaching 0.1 $fTHz^{-1/2}$ (roughly the limit set by body noise) and a polarizing field of at least 0.1T. Both are achievable, but not trivially. A noise of 0.1 $fTHz^{-1/2}$ is at the limit of what one can detect with an appropriate coil size and a SQUID at 4.2K, and assumes that environmental noise can be reduced to this level. Generating a pulsed magnetic field of, say, 0.15T at the prostate or head that can be turned off in some milliseconds is achievable but requires a water-cooled coil and a power supply providing at least 50kW. Screening out external electrical and magnetic interference, almost certainly with a shielded room, presents a major challenge. When the polarizing field is switched off, large eddy currents in the room can severely distort both B_0 and pulsed gradient fields unless one either cancels the field with a second, counter-wound coil or designs a room that rapidly damps out low-frequency current while retaining a high degree of screening at the imaging frequency. Perseverance by the community will undoubtedly achieve these goals.

Another issue concerns cryogenics. I believe the clinical community is unlikely to embrace a system that requires refilling with liquid helium every few days. Fortunately, reliable cryocoolers are readily available at reasonable cost, and ULF MRI has already been demonstrated with a cryocooled SQUID. An alternative approach would be a refrigerator that automatically refills the cryostat at night.

Finally, one should not underestimate the time and cost required for clinical trials. To undertake a meaningful trial will require a company with deep pockets and, one hopes, a steady stream of federal funding.

The group at Los Alamos National Laboratory has been a major driving force in the development of ULF MRI. Their efforts are reflected in this book, which covers all aspects of the subject in depth, ranging from history and the nuts-and-bolts practicalities of building such a system to ULF resonance phenomena and applications of a variety of imaging techniques to pulse sequences and direct neural current imaging. The book is surely destined to become the standard reference in the field.

John Clarke
Berkeley
May 12, 2011

PREFACE

This book endeavors to provide the background for and current status of the emerging field of ultra-low field (ULF) magnetic resonance imaging (MRI). We lay the groundwork by providing a brief history of MRI at extremely low fields and for why ULF NMR and MRI are of both scientific and practical interest. In particular, we examine the benefits realized at applied magnetic fields that are many orders of magnitude below traditional NMR and MRI. We balance the benefits at ULF with the various anticipated and unanticipated challenges our team and others working in the field have experienced, and a variety of approaches used to deal with these challenges. We present the current status in sufficient detail for the reader to effectively pursue ULF MRI investigations in both medical and material science applications. While the primary focus of this book is MRI, we discuss a variety of nuclear magnetic resonance (NMR) phenomena, particularly as they apply at ULF, because ultimately MRI is simply a spatially encoded measurement of specific NMR phenomena.

Traditional MRI involves applied magnetic fields typically in the Tesla regime. Most clinical imaging instrumentation operates at 1.5T, with more 3T imagers being installed every day. The lowest magnetic fields commonly used in clinical instruments are 0.3T (3kG) in applications where an open geometry is required and lower spatial resolution is acceptable or tolerable. Exploring NMR signals at extremely low fields in the milli-Tesla regime was initially reported about two decades ago, where the NMR signal for water was observed at 10mT. However, it has been only in the last decade or so since the observation of exceptionally narrow NMR line widths for various liquid solutions at a few micro-Tesla was reported. The field of ULF NMR and MRI has seen a tremendous growth of publications and research investment around the world since then. This book describes the current state of the art of ULF MRI in our laboratory and others, and while we make an effort to be thorough and relatively complete, the field is evolving rapidly and new ideas are constantly being pursued and reported. We will share practical insights into ideas being pursued and conclude the book with a number of promising concepts for ULF applications that have yet to be investigated and are, as yet, unproven.

Our book focuses on the practical aspects of ULF MRI that will enable the reader to practice in the field. Only a few of the most relevant derivations of first principles of ULF NMR and MRI are provided, with a focus on those specifically relevant to the regime of ULF (e.g., concomitant gradients) and those we thought were lacking elsewhere. Others are provided in the bibliography. We attempt to present a thorough discussion of concomitant gradients because of the large effect they can have on MRI at ULF. While they have been mentioned in high field MRI texts, concomitant gradients have been either treated with simple approximations or entirely ignored.

We present a detailed discussion of current state-of-the-art instrumentation that is unique to ULF MRI. The most common sensor to acquire the NMR signal for ULF MRI is the superconducting quantum interference device (SQUID). SQUIDs are the most sensitive magnetic field sensors in wide use today but require cooling with liquid cryogens (liquid nitrogen or liquid helium). Furthermore, SQUIDs require extraordinary expertise and measures to operate in a typical ULF MRI environment. While we thoroughly cover the techniques needed to employ SQUID sensors in ULF MRI, we also discuss the ongoing search for robust, noncryogenic sensors with the required sensitivity to the desired signal. We present the tradeoffs for currently available sensors. Our discussion of the instrumentation also includes all other aspects of the hardware used in ULF MRI systems, together with experimental techniques and practical insights into how it all works.

We have interspersed relatively general material throughout the book to provide a complete and self-consistent picture for the reader, but we also rely heavily on many excellent references and readily available sources as needed to provide a comprehensive picture of the field. We have made an effort to carefully define nomenclature and thoroughly describe methods to avoid the confusion that can occur between the many sources of NMR information, particularly as one switches between high-field and ULF MRI. A comprehensive table of acronyms and abbreviations is also provided.

Working at the forefront of a new field is exhilarating, educational, and competitive. Many novel features and capabilities of ULF MRI have been discovered, yet we are certain that only the proverbial surface of the field has been scratched. There is far more yet to be discovered and learned, and we wish you, the reader, the very best of luck and insight.

Robert H. Kraus Jr.
Michelle A. Espy
Per E. Magnelind
Petr L. Volegov

ACKNOWLEDGMENTS

We wish to acknowledge the Los Alamos National Laboratory (Los Alamos National Security, LLC) for the research support through the Laboratory Directed Research and Development program, the National Institutes of Health, and the U.S. Department of Homeland Security. In addition, one of us (RHK) wishes to thank Samitaur Medical Technologies and to acknowledge the support and interest of the principals of SMT in advancing medical technology for all humanity. We would also like to thank the many people with whom we have had stimulating and insightful discussions regarding this book. While there are far too many people to individually name here, we would like to specifically acknowledge Prof. John Clarke, Prof. Martin Burghoff, Prof. Risto Ilmoniemi, Ms. Miranda Intrator, Prof. Stefan Posse, Dr. John George, Dr. John Mosher, Dr. Leon Heller, Dr. Don Tucker, Dr. Sergei Turovets, Dr. Jaakko Nieminen, Dr. Rainer Körber, and Mr. Shaun Newman for their many valuable insights, critiques, suggestions, and contributions during the preparation of this book.

We must also acknowledge the many members of our research team (fondly known as the "SQUID Team"), past and present, who have contributed so much to the field of ULF MRI and biomagnetism.

We also wish to make a special acknowledgement and express our sincere appreciation to our colleague Dr. Andrei Matlashov for his critical role in all aspects of the Los Alamos experimental capability in ULF NMR and MRI. Without him, we certainly wouldn't have had much to write about!

Finally, there can be no acknowledgement or "thank you" sufficient to express the gratitude and appreciation we feel for those most important to us: our families, who have sacrificed countless hours for the sake of this book.

COMMON ACRONYMS AND ABBREVIATIONS

We include a list of common acronyms, abbreviations, and symbols used in this book. We ask the reader to be aware that sections of the book where detailed mathematical derivations are presented may use symbols and letters in formulae that are not consistent with this table. We have, however, attempted to clearly define every symbol and character at the first instance of use in the context of the derivation.

2D	Two-dimensional
3D	Three-dimensional
A	Context dependent: Amp or Nuclear mass number (number of protons and neutrons in a given nucleus)
Å	Ångström, 10^{-10}m
AC	Alternating current (time-varying current)
ADC	Analog-to-Digital converter
AM	Atomic Magnetometer (or Atomic Magnetometry)
ASL	Arterial spin labeling, a MRI technique used to measure blood flow that can be used to deduce brain function
B_0	MRI magnetic field, typically both the polarization and measurement field used in high-field MRI
B_m	Measurement magnetic field
BOLD	Blood Oxygen Level Dependent, a MRI technique used to deduce brain activity
B_p	Polarization magnetic field used in MRI.
BW	Bandwidth
CNR	Contrast-to-noise ratio
CSF	Cereberal spinal fluid
DC	Direct current (constant current)
DNI	Direct neural imaging, a method to directly measure the neural activity (presumably in the brain). Our team coined the acronym to refer to the direct imaging of neural currents using ULF MR

e	Elementary charge
EEG	Electroencephalography
EIT	Electrical impedance tomography
EPI	Echo-planar imaging
f	Frequency, when used as a variable or quantity, typically in Hz.
FAIR	Flow-sensitive alternating inversion recovery, a MRI technique to used to measure blood flow that may be associated with function
FC	Field cycling, typically refers to techniques for varying the NMR or MR field
FFT	Fourier Transform (or Fast Fourier Transform)
FID	Free Induction Decay
FLAIR	Fluid attenuated inversion recovery
FLASH	Fast low-angle shot
fMRI	Functional magnetic resonance imaging
FOV	Field-of-view, often (thought not always) synonymous with volume of interest
G	(non-italicized) Gauss, unit of magnetic field equal to 10^{-4} T
G	Magnetic field gradient (usually includes a direction: G_x, G_y, G_z).
GMR	Giant magneto-resistive or giant magnetoresistance
h	Planck's constant (6.626×10^{-34} J-sec)
H	Magnetic field strength
$\hbar$	$h/2\pi$ or the reduced Planck's constant (1.055×10^{-34} J-sec)
HF	High Field, typically referring to >0.3 T imaging field in HF MRI
HTC	High (critical temperature) superconductor, typically designates materials with superconducting critical temperature well above ~4 K. also high-T_c
Hz	Hertz, cycles per second
I	Context dependent: Current or spin quantum number
J	Current density
J	(non-italicized) Joule
k	The mathematical space convient for imaging, "k-space"
K	Kelvin
k_B	Boltzmann's constant (1.381×10^{-23} J/K)
L	Inductance (also used as image size in Ch. 4 derivations)
LANL	Los Alamos National Laboratory
LF	Low (magnetic) Field, commonly referring to MRI fields below 0.3T. We define LF MRI as the regime between ULF MRI and HF MRI.
LHe	Liquid helium
LN	Liquid Nitrogen
LSB	Least Significant Bit, the lowest significant bit in a digital acquisition system
LTC	Low (critical temperature) superconductor, typically ~4 K and below. Also low-T_c

M	Magnetization, may be a vector (**M**) quantity, scalar (*M*) or a vector component (e.g. M_x)
MAGVIZ	The name given to the ULF MR relaxometry technique used to differentiate materials based on relaxation profile
MEG	Magnetoencephalography
MR	Magnetic Resonance
MREIT	Magnetic Resonance electrical impedance tomography
MRI	Magnetic Resonance Imaging
MSR	Magnetically Shielded Room
N	Number in a given population (such as number of spins)
nc-MRI	Neural current MRI—designates methodologies used in MRI to detect signatures directly associated with neural activity (such as rapid dephasing).
NEMA	National Electrical Manufacturers Association, See also www.nema.org
NMR	Nuclear Magnetic Resonance
NQR	Nuclear quadrupole resonance
PET	Positron emission tomography (medical imaging modality using radioisotopes)
PSD	Power Spectral Density
R	Resistance
Rad	Radian
RF	Radio frequency, often referred to as "rf" elsewhere
RFI	Radio frequency interference
ROI	Region of Interest (see VOI/volume of interest)
S	Context dependent: Shielding factor (various subscripts designate specific type), or the NMR signal measured from a specific region or volume.
SD	Standard deviation
SENSE	Sensitivity Encoding – a method for using multiple sensor to improve imaging speed or signal-to-noise
SMASH	Simultaneous acquisition of spatial harmonics—a method for using multiple sensor to improve imaging speed
SNR	Signal-to-noise ratio
SOC	Streams of commerce, refers to commonly available packaging of commodities
Spin	Quantum mechanical spin, typically referring to nuclear spin in this book
SQUID	Superconducting Quantum Interference Device
T	(non-italicized), Tesla, unit of magnetic field equal to 10,000 G
T	Context dependent: Temperature or time when used as a variable
t	Typically refers to a time, often denoted by a subscript (e.g. t_g – time gradient field is applied, t_a – acquisition time, etc.)
T_1	Longitudinal (or spin-lattice) relaxation time
T_2	Transverse (or spin-spin) relaxation time

T_c	Critical temperature, typically referring to the temperature at which a material becomes superconducting
ULF	Ultra-low magnetic field (erroneously "ultra-low frequency")
V	(Context dependent) Voltage or Volume
VOI	Volume of interest, typically the imaging region of interest in MRI
Voxel	Volume element, typically referring to a specific size element from which a signal is derived
Z	(non-italicized) refers to the nuclear atomic number
Z	Impedance
μ_0	Free space permeability
γ	Gyromagnetic ratio (depends on isotope/nucleus)
μ	Relative permeability
μ-metal	Mu-metal, generally refers to any high magnetic permeability material
δ	Skin depth—the thickness of a material needed to reduce a signal by $1/e$
σ	Electrical conductivity
χ	Magnetic susceptibility
Ω	Ohm, measure of resistance
ω	Frequency (general)
ω_L	Larmor Frequency

ULTRA-LOW FIELD NUCLEAR MAGNETIC RESONANCE

CHAPTER 1

FUNDAMENTAL PRINCIPLES OF NMR AND MRI AT ULF

1.1 INTRODUCTION

Magnetic resonance imaging (MRI, originally called nuclear magnetic resonance [NMR] imaging) has for nearly four decades been a tool synonymous with high-tech and high-resolution imaging [1]. While MRI applications are most widely known in the medical field [2], applications are also many and varied outside the medical community. A few examples include anthropology [3], paleontology [4], evolution [5,6], material analysis [7,8], and analyzing food quality and safety [9–11]. Widely known for its medical diagnostic capability, MRI is also a powerful research tool because of a wide variety of unique capabilities that include high resolution, localized spectroscopy, isotopic specificity, etc. The popularity of MRI in general, and in comparison to x-ray–based imaging methods in particular, has also been bolstered by the fact that it employs no ionizing radiation and that MRI can often differentiate materials with virtually identical density and chemical composition (called "contrast"). For example, soft tissue contrast that can differentiate white and gray matter in the brain is commonplace for MRI while virtually beyond the capability of x-ray. While the number and breadth of MRI techniques and applications have exploded in the four short decades since Lauterbur and Mansfield demonstrated the method in the 1970s, the field has driven to ever-higher magnetic fields in the quest for more signal, better signal-to-noise ratios (SNRs), and ever-greater spatial resolution. This book provides the rationale and the techniques for applications in which bigger may not always be better.

At the heart of all MRI is the NMR signal. In the simplest form, an MRI is constructed as a spin density (typically for protons in most MRI applications) image. This is referred to as a "proton density-weighted" (or "spin density-weighted") image. For example, because the proton spin density in tissue is far greater than bone, a large spin density signal is generated by tissue and a correspondingly small signal from bone. Figure 1.1 illustrates a single-slice MRI for a human hand derived primarily from the proton spin density where the brightness (lighter regions of the image) indicates the density of protons in a given volume of the image. The area around the hand (i.e., air) has little or no proton spin density whereas the tissue (flesh) has a significant proton population. The dark gaps in the fingers occur at the joints and are the result of the short relaxation time of the cartilage. This difference is known as T_2 contrast, a concept we will discuss later.

Anatomical images are typically generated by exploiting the differences, often quite small, in NMR signal between various tissue types (e.g., white vs. gray matter) and

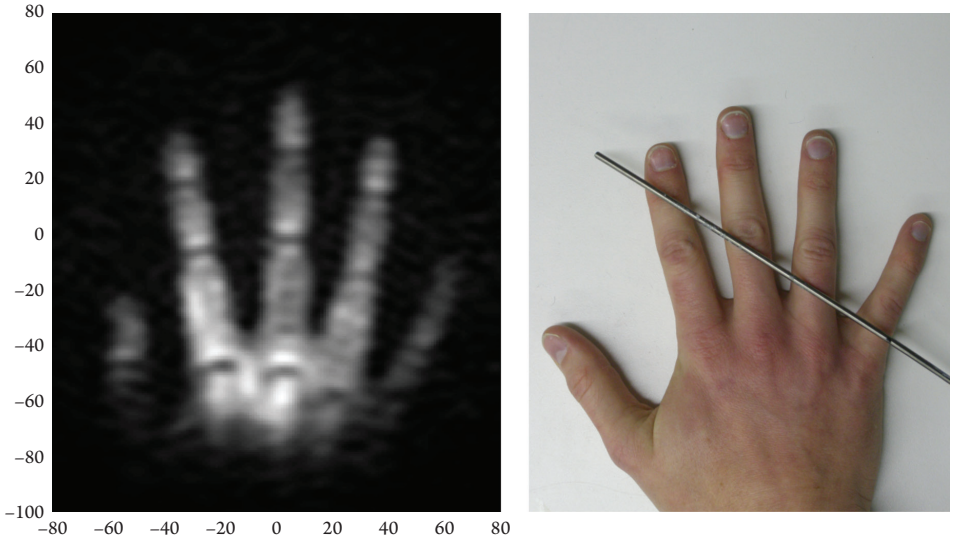

FIGURE 1.1 (Left) MRI of hand at ULF with Ti rod. The image is primarily a proton density-weighted image where brightness is roughly a measure of proton density. The proton spin density weighted MR image was acquired at 94μT after pre-polarization at 30mT with a spatial resolution of approximately 2mm. While the left panel is a simple MRI acquired at ULF, it is extraordinary because it could not have been acquired in a typical MRI scanner due to the presence of the Ti rod. (Right) Photograph of the hand for which the MRI was acquired, showing a 4mm-diameter titanium rod that was placed on top of the hand during acquisition of the ULF MRI. The presence of such metal in typical MRI scanner would have made the acquisition of the MRI in the left panel virtually impossible, as we shall describe later in the book.

fluids (e.g., blood, cerebrospinal fluid [CSF], etc.). Imaging human tissue most commonly exploits the difference between tissue parameters of spin density (e.g., Fig. 1.1), spin-lattice relaxation, spin-spin relaxation, flow, and diffusion. MRI in other applications relies on the same basic techniques where differences in a specific NMR phenomenon are imaged and associated with specific material type. For example, imaging fat content in meat relies on the fact that the spin density and relaxation times in fat are significantly different than other tissue types. These differences in NMR phenomena result in a contrast or difference between materials and tissue types that can be exploited with the appropriate techniques to generate the desired image.

Contrast can (and often is) a very dynamic phenomenon, changing with time as a consequence of the inherent NMR phenomena themselves or as a result of physiological processes. In recent years, MRI has been applied to observe the temporal evolution of NMR signals/signatures combined with the spatial information. One of the most common and powerful examples of this method is functional MRI (fMRI), in which the time evolution of blood oxygenation, blood flow, and blood volume as a function of location have been used to deduce function in the human brain [12]. While fMRI has become an exceptionally powerful tool, it is still limited by temporal resolution and an indirect association with the underlying neural activity. Nevertheless fMRI has provided an unprecedented map of the functional architecture of the cortical areas that are the substrate of higher brain function.

The differences in the NMR signal for the various tissue types and fluids are spatially encoded through the application of magnetic field gradients. The final MRI image is developed from the analysis of the resulting signal (described later in the book and in references [13,14]) acquired by a variety of possible sensors. The specific NMR phenomenon (e.g., relaxation time, spin diffusion, etc.) imaged is elicited by the specific pulse sequence applied. These are discussed in detail later in the book.

Improving spatial resolution, reducing imaging time, and increasing the sensitivity to differences between materials (e.g., tissue types, fluids, etc.) are the key drivers in the scientific and technological advancement of MRI. A common need in each of these key drivers is ever-greater signal from a given volume of the sample (or voxel) and the SNR to differentiate one voxel from its neighboring voxels. We will briefly examine here the primary contributing factors to the NMR signal that underpins the MRI and the relationships to variables, particularly those that can be controlled by the imaging system. Noise is a more complex topic and will be covered in later chapters. Suffice it to say that the quest for ever-greater signal has driven most of the advances in MRI over the last few decades.

The phenomenon that underlies NMR is the rotation of nuclear magnetic (dipole) moments about a magnetic field. While it is not feasible to detect the rotation of a single nucleus, the NMR signal observed in spectroscopic NMR and MRI arises from a population of nuclei, similarly aligned and rotating in phase about a magnetic field that is roughly uniform across the sample. Because the nuclear magnetic moment, μ, is proportional to the nuclear spin, S, every nucleus with non-zero spin can produce a NMR signal. While virtually every known element has an isotope (isotopes for a given element have the same "Z" or number of protons in the nucleus but differing number of neutrons and consequently atomic mass number "A") that has a non-zero spin, only a handful are commonly used in NMR and even fewer in MRI. The vast majority of MRI is based on the NMR signal of the proton (^{1}H, the most abundant form of hydrogen) because the magnitude of the NMR signal per nucleus (the NMR "sensitivity," see Table 1.1) is larger for ^{1}H than any other known isotope. Furthermore, hydrogen is the most abundant element in the human body (measured as number of nuclei). Water makes up approximately 75% of the human body and every water molecule includes two hydrogen nuclei, not to mention the hydrogen contained in fats and proteins. Consequently, there are more hydrogen nuclei in the human body with which to generate the observed NMR signal.

Traditional MRI involves applied magnetic fields typically in the Tesla (T) regime. Most modern clinical imaging instrumentation operate at 1.5T to 3T. The lower extreme of magnetic fields commonly used in clinical instruments, the so-called "low-field" regime, is 0.2T to 0.3T (3kG). These instruments are commonly used in applications where an open geometry is required and lower spatial resolution is acceptable or tolerable. In general, the MRI technology is moving toward ever-larger magnetic fields, with more 3T clinical imagers being installed every day. The primary driver for this trend toward increasing magnetic fields is the increased signal realized as a function of the applied "polarizing" field, which results in faster imaging and higher resolution, along with other benefits that result with more signal. However, these larger fields come at a cost, monetary and otherwise. Larger fields require physically larger and heavier magnets that place ever-increasing demands on the facility to house these instruments. Increasing MRI fields also result in numerous safety challenges that become more severe with increasing fields. We compare various aspects of high- and low-field MRI in more detail later.

The development of "low-field" (LF) MRI systems in the 1980s thorough the early 21st century were initially driven by the desire to reduce patient anxiety by enabling open-magnet designs, as opposed to the physically constraining cylindrical design of most high-field